SUPPORTING INFORMATION

Mimicking the secretory action of a gland by a composite system made of a pH-responsive surfactant-based hydrogel and a dialysis membrane.

Alessio Cesaretti,[a] Irene Di Guida,[a] Naishka E. Caldero-Rodríguez,[a,b] Catia Clementi,[a] Raimondo Germani,[a] Pier Luigi Gentili*,[a]

[a]Department of Chemistry, Biology and Biotechnology, University of Perugia,

Via Elce di sotto 8, 06123 Perugia, Italy

[b]Department of Chemistry, College of Natural Science, University of Puerto Rico, Río Piedras Campus, San Juan, PR 00931-3346.

*E-mail: pierluigi.gentili@unipg.it

Contents **Page**

I. Results

*I.1 Interactions between **pDoAO** and **ARS***

The equation for the determination of the equilibrium association constant [1] between **ARS** and the micelles of **pDoAO** is:

$$\frac{1}{A - A_0} = \frac{1}{(A_\infty - A_0)K([pDoAO] - cmc)} + \frac{1}{A_\infty - A_0} \quad (1)$$

where A is the absorbance when the concentration of the micelles is equal to the difference (***[pDoAO]-cmc***), A_0 is the absorbance before any addition of the surfactant, and A_∞ is the absorbance when all the **ARS** molecules are associated with the micelles.

I.1.1 Titrations of ARS with pDoAO at pH=7.5

The titration of 2 mL of a buffered **ARS** solution (8.0×10^{-5} M) at pH=7.5, has been performed in a fluorimetric cuvette by adding increasing microvolumes of a buffered **pDoAO** solution ($C_0 = 1.0 \times 10^{-3}$ M) at pH=7.5. The spectral evolution recorded for this titration is shown in Figure 1B. The composition of the solution after each addition is reported in Table S1.

Table S1. Composition of the solution of **ARS** at pH=7.5, after each addition of **pDoAO**.

n° addition	**Total added volume (µL)**	**[pDoAO] (M)**	**moles(pDoAO)/ moles(ARS)**	**[micelles]/[ARS]**
1	3	1.5×10^{-6}	0.019	/
2	8	4.0×10^{-6}	0.05	/
3	15	7.4×10^{-6}	0.09	/
4	25	1.2×10^{-5}	0.16	/
5	40	2.0×10^{-5}	0.25	0.051
6	60	2.9×10^{-5}	0.38	0.17
7	80	3.8×10^{-5}	0.50	0.29
8	100	4.8×10^{-5}	0.63	0.42
9	120	5.7×10^{-5}	0.75	0.54
10	150	7.0×10^{-5}	0.94	0.73
11	180	8.3×10^{-5}	1.13	0.91
12	210	9.5×10^{-5}	1.31	1.09
13	240	1.1×10^{-4}	1.5	1.32
14	280	1.2×10^{-4}	1.75	1.48
15	325	1.4×10^{-4}	2.03	1.80
16	375	1.6×10^{-4}	2.34	2.14
17	435	1.8×10^{-4}	2.72	2.50
18	505	2.0×10^{-4}	3.16	2.88

19	590	2.3×10^{-4}	3.69	3.46
20	690	2.6×10^{-4}	4.31	4.10
21	800	2.9×10^{-4}	5	4.80
22	920	3.2×10^{-4}	5.75	5.55
23	1050	3.4×10^{-4}	6.56	6.18
24	1190	3.7×10^{-4}	7.44	7.06
25	1340	4.0×10^{-4}	8.38	8.04
26	1400	4.1×10^{-4}	8.75	8.37
27	1600	4.5×10^{-4}	10.2	9.82
28	1820	4.8×10^{-4}	11.6	11.2
29	2060	5.1×10^{-4}	13.1	12.7
30	2320	5.5×10^{-4}	15.0	14.6

Determination of the association constant between ARS and micelles at pH=7.5

Determination of the association constant K of the di-anionic form of **ARS** to the **pDoAO** micelles in an aqueous solution buffered at pH=7.5. The values of absorbance refer to λ=495 nm that is the wavelength of the maximum for **ARS** in water at pH=7.5. The red straight line represents the fitting function presented in equation (1).

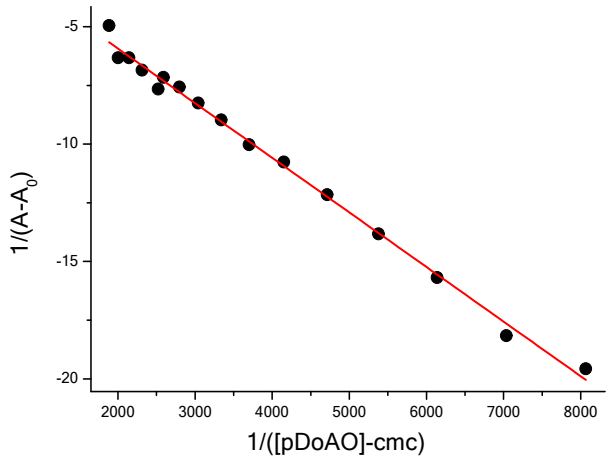

Figure S1. Application of equation (1) to the corrected spectral data collected at 495 nm, for **ARS** (8.0×10^{-5} M) and [**pDoAO**] ranging from 1.40×10^{-4} M to 5.46×10^{-4} M. The A values have been corrected by considering the dilution effect due to the successive additions of **pDoAO** solution.

I.1.2 Titrations of ARS with pDoAO at pH=3.1

The titration of 2 mL of a buffered **ARS** solution (5.8×10^{-5} M), has been carried out in a fluorimetric cuvette by adding increasing microvolumes of a **pDoAO** solution ($C_0=9.7\times10^{-4}$ M) at pH=3.1. The spectral evolution recorded for this titration is shown in Figure 1C. The composition of the solution after each addition is reported in Table S2.

Table S2. Composition of the solution of **ARS** at pH=3.1, after each addition of pDoAO.

n° addition	**Total added volume (µL)**	**[pDoAO] (M)**	**moles(pDoAO)/ moles(ARS)**	**[micelles]/[ARS]**
1	3	1.5×10^{-6}	0.026	/
2	8	3.9×10^{-6}	0.067	/
3	15	7.2×10^{-6}	0.125	/
4	25	1.2×10^{-5}	0.21	/
5	40	1.9×10^{-5} > cmc	0.33	0.07
6	60	2.8×10^{-5}	0.50	0.23
7	80	3.7×10^{-5}	0.67	0.39
8	100	4.6×10^{-5}	0.83	0.56
9	120	5.5×10^{-5}	1.00	0.73
10	150	6.8×10^{-5}	1.26	0.98
11	180	8.0×10^{-5}	1.50	1.22
12	210	9.2×10^{-5}	1.75	1.47
13	240	1.04×10^{-4}	2.01	1.72
14	280	1.19×10^{-4}	2.34	2.05
15	325	1.36×10^{-4}	2.73	2.42
16	375	1.53×10^{-4}	3.13	2.83
17	435	1.73×10^{-4}	3.64	3.32
18	505	1.96×10^{-4}	4.22	3.91
19	590	2.21×10^{-4}	4.93	4.60
20	690	2.49×10^{-4}	5.77	5.43
21	800	2.77×10^{-4}	6.69	6.32
22	920	3.06×10^{-4}	7.69	7.33

23	1050	3.34×10^{-4}	8.78	8.39
24	1190	3.62×10^{-4}	9.96	9.54
25	1340	3.89×10^{-4}	11.20	10.77
26	1400	3.99×10^{-4}	11.71	11.26

Determination of the association constant between ARS and micelles at pH=3.1.

Determination of the association constant K of the mono-anionic form of **ARS** to the **pDoAO** micelles in an aqueous solution buffered at pH=3.1. The values of absorbance refer to λ=420 nm, which is the wavelength of the maximum for **ARS** in water at pH=3.1. The red straight line represents the fitting function presented in equation (1).

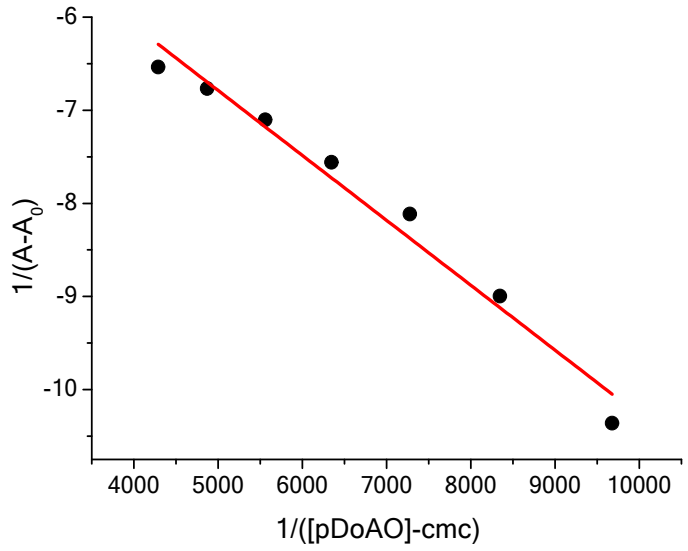

Figure S2. Application of equation (1) to the corrected spectral data collected at 420 nm, for **ARS** (5.8×10^{-5} M) and [**pDoAO**] ranging from 1.19×10^{-4} M to 2.49×10^{-4} M. The A values have been corrected by considering the dilution effect due to the successive additions of **pDoAO** solution.

I.1.3 Titrations of ARS with pDoAO in pure unbuffered water (initial pH=5.5).

The titration of 2 mL of **ARS** 5.4×10^{-5} M in pure unbuffered water, having the initial pH equal to 5.5, has been carried out in a fluorimetric cuvette by adding increasing microvolumes of a **pDoAO**

unbuffered water solution (C_0=9.8×10^{-4} M). The spectral evolution recorded for this titration is shown in Figure 1D. The composition of the solution after each addition is reported in Table S3.

Table S3. Composition of the solution of **ARS** in pure water, after each addition of **pDoAO**.

n° addition	**Total added volume (µL)**	**[pDoAO] (M)**	**moles(pDoAO)/ moles(ARS)**	**[micelles]/[ARS]**
1	3	1.5×10^{-6}	0.027	/
2	8	3.9×10^{-6}	0.073	/
3	15	7.3×10^{-6}	0.136	/
4	25	1.2×10^{-5}	0.227	/
5	40	1.9×10^{-5} > cmc	0.36	0.06
6	60	2.85×10^{-5}	0.54	0.24
7	80	3.77×10^{-5}	0.73	0.42
8	100	4.67×10^{-5}	0.91	0.60
9	120	5.55×10^{-5}	1.09	0.78
10	150	6.84×10^{-5}	1.36	1.04
11	180	8.1×10^{-5}	1.63	1.31
12	210	9.3×10^{-5}	1.91	1.58
13	240	1.05×10^{-4}	2.18	1.85
14	280	1.20×10^{-4}	2.54	2.20
15	325	1.37×10^{-4}	2.95	2.60
16	375	1.55×10^{-4}	3.40	2.99
17	435	1.75×10^{-4}	3.95	3.58
18	505	1.98×10^{-4}	4.58	4.22
19	590	2.23×10^{-4}	5.18	4.96
20	690	2.51×10^{-4}	6.26	5.85
21	800	2.80×10^{-4}	7.26	6.84
22	920	3.09×10^{-4}	8.35	7.92
23	1050	3.37×10^{-4}	9.53	9.07

Determination of the association constant between ARS and micelles in pure unbuffered water.

Determination of the association constant K between **ARS** and **pDoAO** micelles in pure unbuffered water. The values of absorbance refer to λ=600 nm. The red straight line represents the fitting function that corresponds to equation (1).

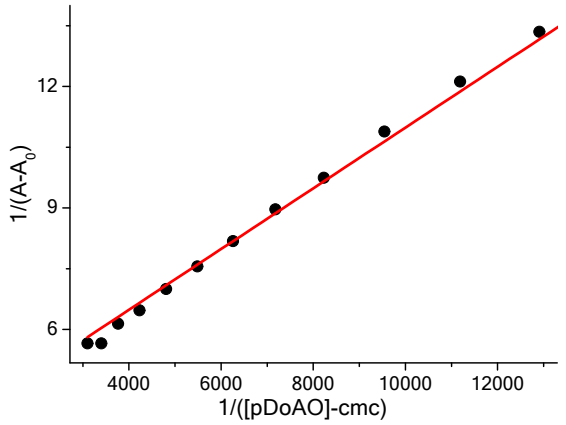

Figure S3. Application of equation (1) to the corrected spectral data collected at 600 nm, for **ARS** (5.4×10^{-5} M) and [**pDoAO**] ranging from 9.3×10^{-5} M to 2.8×10^{-4} M. The A values have been corrected by considering the dilution effect due to the successive additions of **pDoAO** solution.

*I.2 Dependence of **PyI** fluorescence quantum yield on the viscosity of **pDoAO** solutions.*

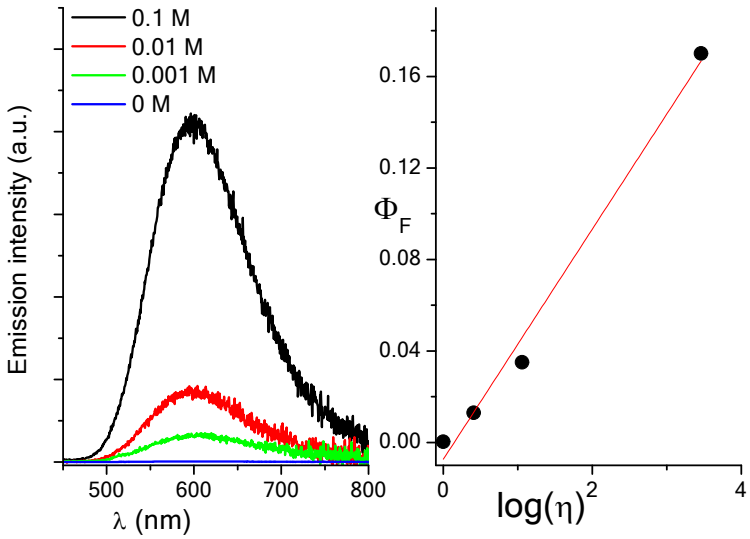

Figure S4. PyI emission spectra at different concentrations of **pDoAO** (read the legend in the plot on the left), and linear trend of Φ_F vs. the logarithm of viscosity (η), on the right. The linear function

represented by the red straight line is $\Phi_F = -(0.074 \pm 0.007) + (0.050 \pm 0.004)\log(\eta)$, determined by the least-squares method.

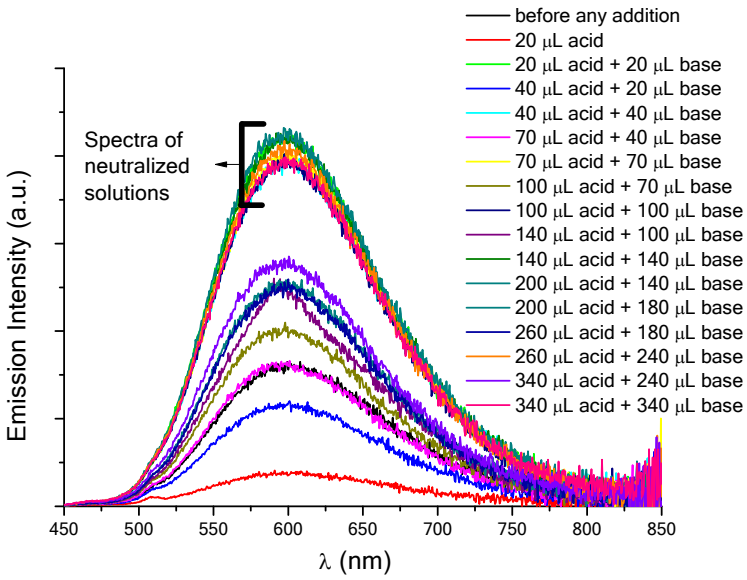

Figure S5. Effect of consecutive injections of HCOOH 1M (acid) and NaOH 1M (base) on the emission spectrum of **PyI** (2×10^{-5} M) dissolved in 2.5 mL solution with [**pDoAO**]=10^{-2} M. The emission spectra have been corrected by the dilution effect. The most intense spectra have been recorded after neutralizing the acid.

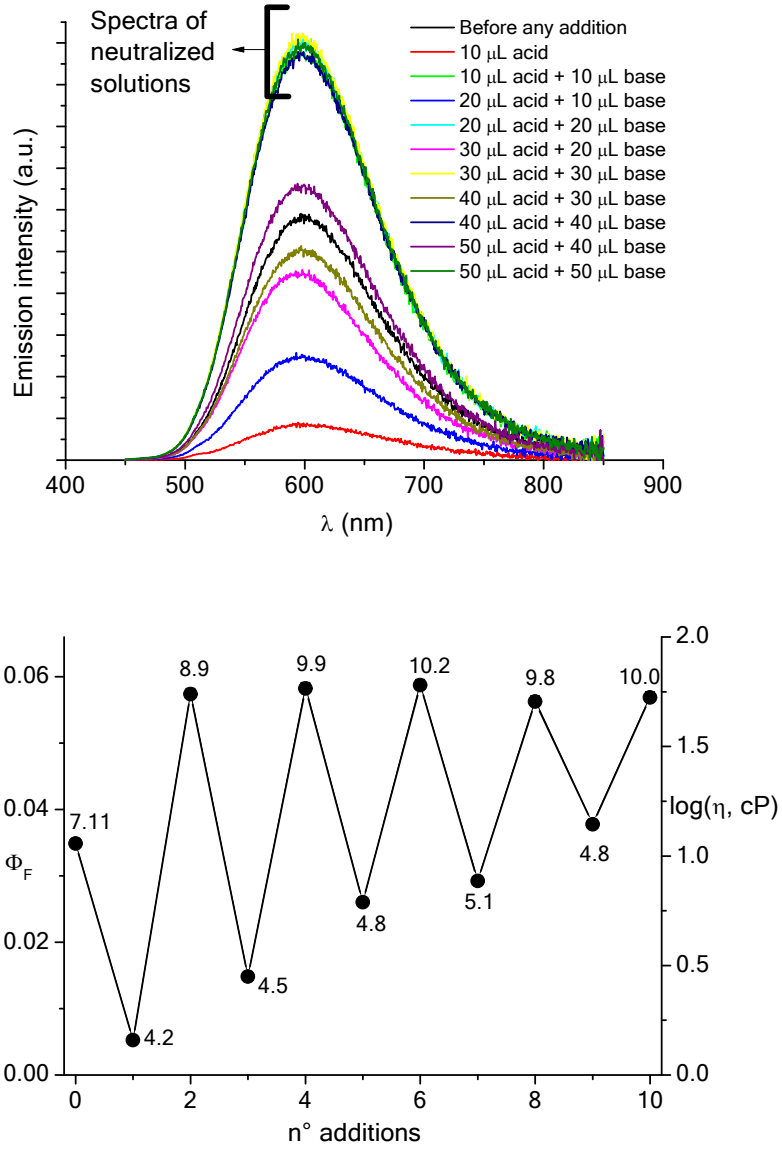

Figure S6. Effect of consecutive injections of HCOOH 1M (acid) and NaOH 1M (base) on the emission spectrum of **PyI** (2×10^{-5} M) dissolved in 2.5 mL solution with [**pDoAO**]=10^{-2} M (upper graph). The emission spectra have been corrected by the dilution effect. The lower graph shows the trend of Φ_F(**PyI**) and the logarithm of the viscosity after every addition of either the acid or the base.

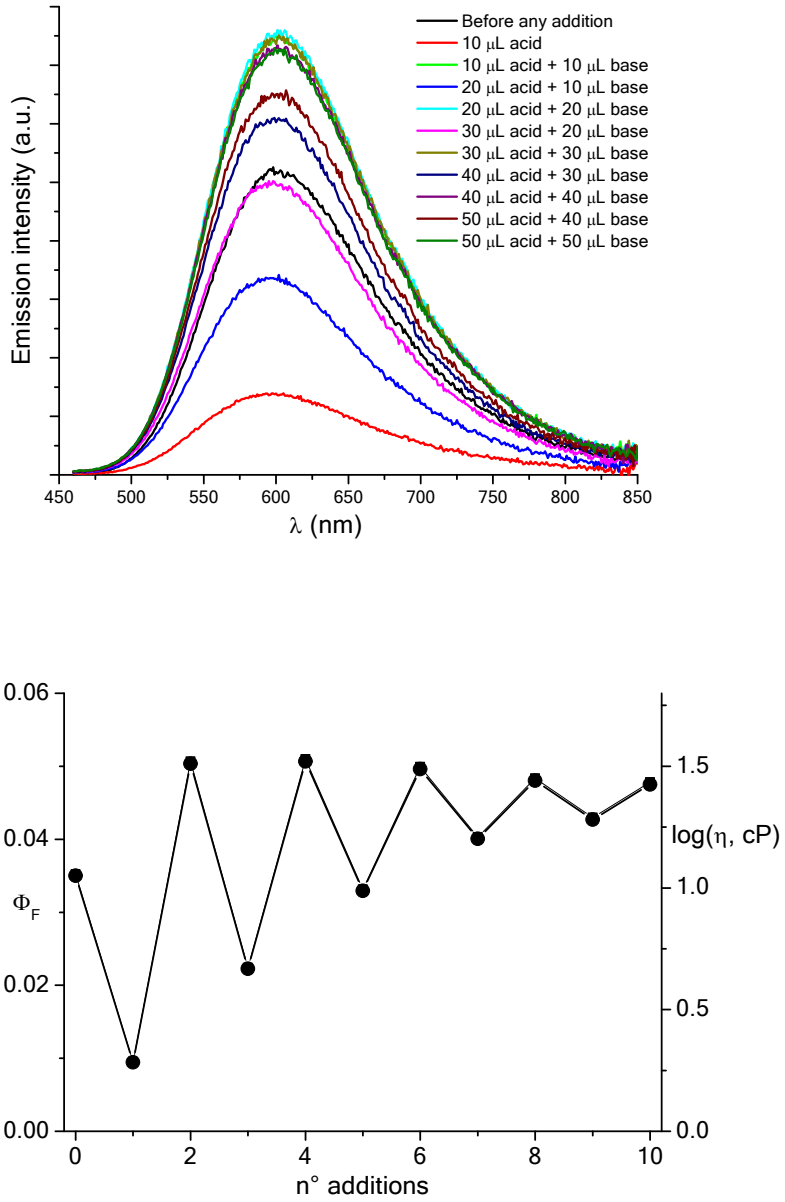

Figure S7. Effect of consecutive injections of HCl 1M (acid) and NaOH 1M (base) on the emission spectrum of **PyI** (2×10^{-5} M) dissolved in 2.5 mL solution with [**pDoAO**]=10^{-2} M (upper graph). The emission spectra have been corrected by dilution effect. The lower graph shows the trend of Φ_F(**PyI**) and the logarithm of the viscosity after every addition of either the acid or the base.

I.3 Activity of the Artificial Gland

The data shown in Figures 5A and 5B of the Article were obtained by using 1.98 g of the 0.1 M **pDoAO** gel containing **C_8Ac** at the concentration of 8×10^{-6} M. The gel-to-sol transition was induced by adding 19.5 μL of 99% CH_3SO_3H to the gel. A volume of 20 mL of pure deionized water

constituted the phase collecting the secretion of the artificial gland model when **pDoAO** was in both its gel and sol state. The values of the **C_8Ac** molar fraction ($\chi_{(C_8Ac)}$) secreted by the artificial gland model in both its gel and sol state (Figure 5A) were determined by recording the emission spectrum of **C_8Ac** from the aqueous solution contained in the beaker. By knowing that the fluorescence quantum yield of **C_8Ac** is $\Phi_F(\lambda_{exc}@360) = 0.32$, and by using tetracene in cyclohexane as fluorometric standard, it was possible to calculate the absorbance of **C_8Ac** (A_{C_8Ac}) through equation (2):

$$A_{C_8Ac} = \frac{Area\ Em(C_8Ac)\ \ \Phi_F(St)}{Area\ Em\ (St)\ \ \Phi_F(C_8Ac)}\left(\frac{n_{aq}}{n_{St}}\right)^2 A_{St} \qquad (2)$$

In (2), St represents the standard; $Area\ Em$ is the integral of the emission spectrum; n_{aq} and n_{St} are the refractive indices of the aqueous and cyclohexane solution, respectively. Then, from the value of A_{C_8Ac}, it was possible to calculate the concentration and $\chi_{(C_8Ac)}$ since the absorption coefficient of **C_8Ac** was known (see Figure S8).

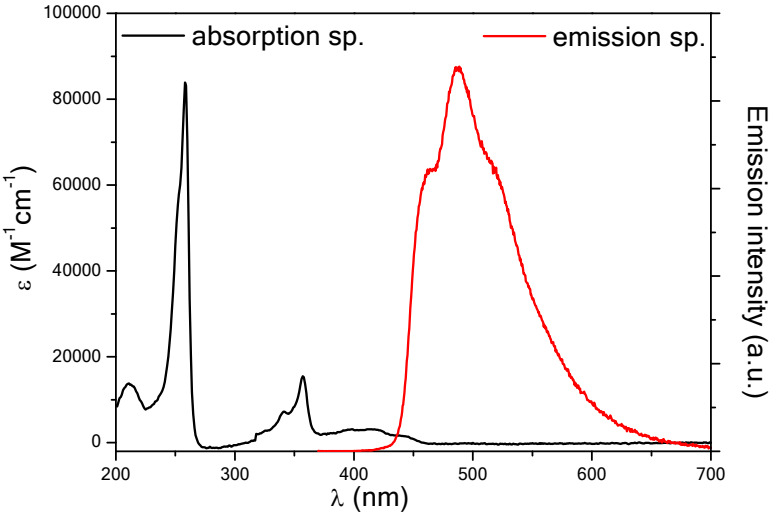

Figure S8. Absorption (black trace) and emission (red trace) spectra of **C_8Ac** in pure water.

The values of the molar fraction of the surfactant molecules ($\chi_{(pDoAO)}$) released by the composite **pDoAO+DM** system was determined by recording the absorption spectra of the aqueous solution and knowing the absorption coefficients values of **pDoAO** molecules in both its zwitterionic and cationic state (see Figure S9).

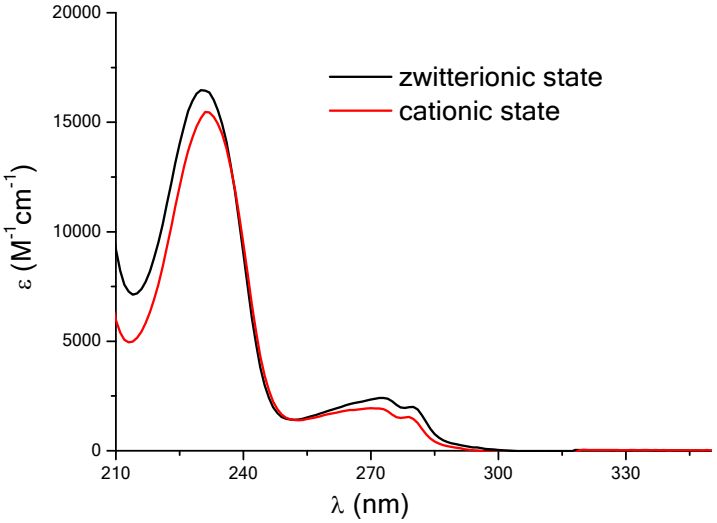

Figure S9. Absorption spectra of **pDoAO** in its zwitterionic (black trace) and cationic (red trace) states.

The emission and absorption spectra of the collecting aqueous solution recorded when **pDoAO+DM** was in the gel state, are shown in Figure S10 and S11, respectively.

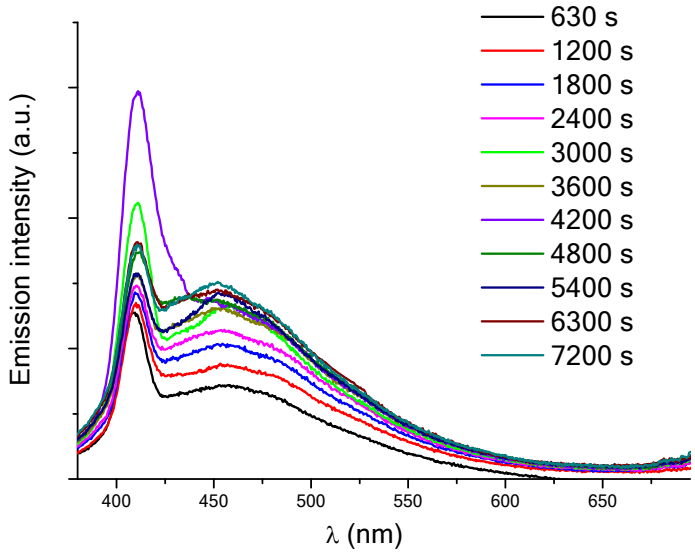

Figure S10. Emission spectra of **C_8Ac** secreted at different elapsed times in the collecting aqueous solution when **pDoAO+DM** is in the gel state.

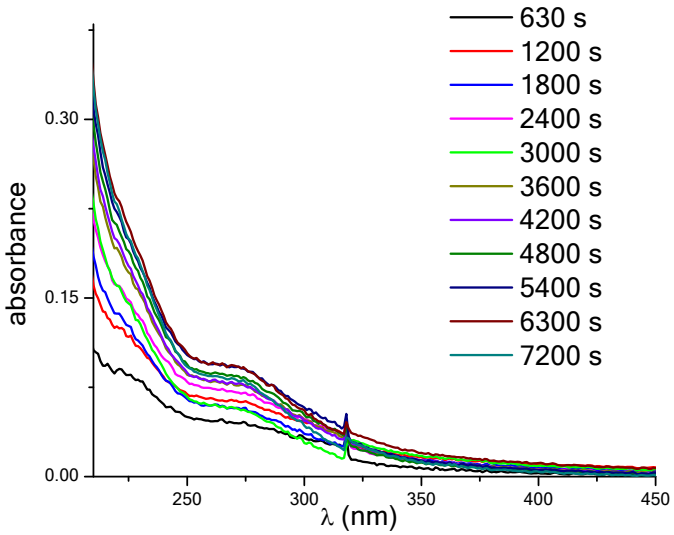

Figure S11. Absorption spectra of the collecting aqueous solution when **pDoAO+DM** is in the gel state.

The emission and absorption spectra of the collecting aqueous solution, recorded when **pDoAO+DM** is in the sol state, are shown in Figure S12 and S13, respectively.

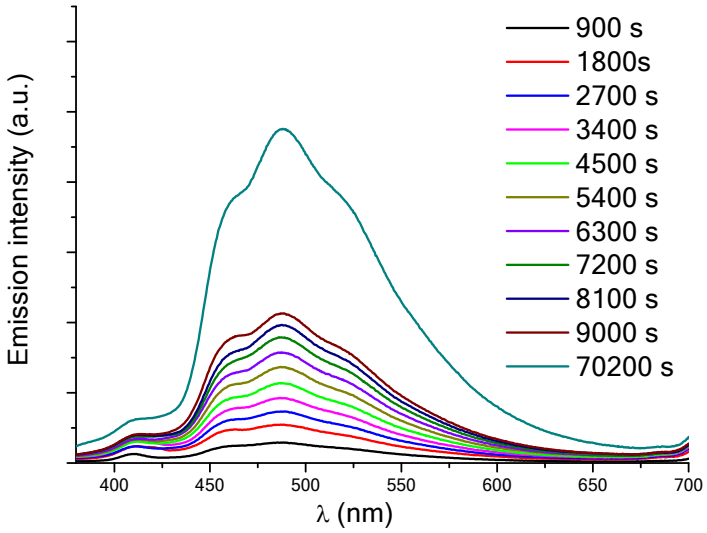

Figure S12. Emission spectra of **C_8Ac** secreted at different elapsed times in the collecting aqueous solution when **pDoAO+DM** is in the sol state.

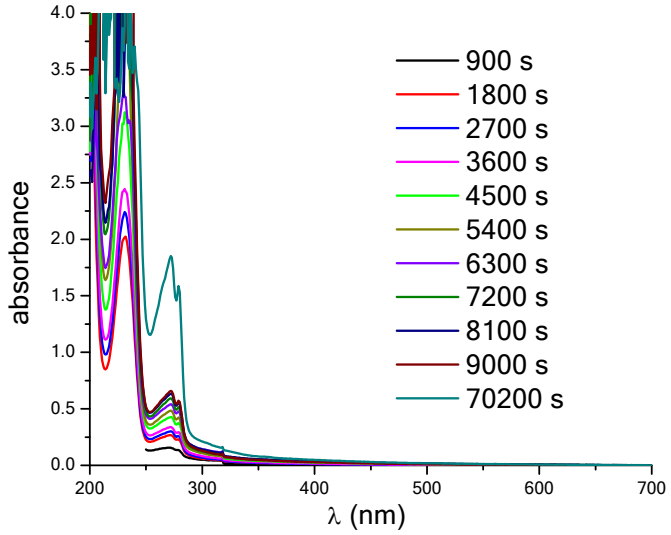

Figure S13. Absorption spectra of the collecting aqueous solution when **pDoAO+DM** is in the sol state.

Table S4. Trends of the concentrations and molar fractions of **C_8Ac** secreted by **pDoAO+DM** from both the gel and the sol state.

Time (s)	[**C_8Ac**] (M) from gel	$\chi_{(C_8Ac)}$ from gel	[**C_8Ac**] (M) from sol	$\chi_{(C_8Ac)}$ from sol
630	1.15×10^{-8}	0,015		
900			5.26×10^{-8}	0,069
1200	1.64×10^{-8}	0,021		
1800	1.92×10^{-8}	0,025	1.04×10^{-7}	0,136
2400	2.11×10^{-8}	0,028		
2700			1.36×10^{-7}	0,179
3000	2.31×10^{-8}	0,030		
3600	2.39×10^{-8}	0,031	1.71×10^{-7}	0,225
4200	2.54×10^{-8}	0,033		
4500			2.07×10^{-7}	0,273
4800	2.53×10^{-8}	0,033		
5400	2.48×10^{-8}	0,033	2.48×10^{-7}	0,327
6300	2.67×10^{-8}	0,035	2.85×10^{-7}	0,375

7200	2.65×10^{-8}	0,035	3.21×10^{-7}	0,423
8100			3.53×10^{-7}	0,464
9000			3.87×10^{-7}	0,509
48000			8.59×10^{-7}	1,130

Table S5. Trends of the concentrations and molar fractions of **pDoAO** released by **pDoAO+DM** from both the gel and the sol state.

Time (s)	[**pDoAO**] (M) from gel	$\chi_{(pDoAO)}$ from gel	[**pDoAO**] (M) from sol	$\chi_{(pDoAO)}$ from sol
630	1.86×10^{-5}	0,00196		
900			8.06×10^{-5}	0,00848
1200	2.59×10^{-5}	0,00272		
1800	2.34×10^{-5}	0,00246	1.39×10^{-4}	0,01466
2400	2.88×10^{-5}	0,00303		
2700			1.57×10^{-4}	0,01654
3000	2.30×10^{-5}	0,00242		
3600	3.19×10^{-5}	0,00336	1.76×10^{-4}	0,01857
4200	3.25×10^{-5}	0,00342		
4500			2.24×10^{-4}	0,02358
4800	3.42×10^{-5}	0,00360		
5400	3.77×10^{-5}	0,00396	2.53×10^{-4}	0,02661
6300	3.77×10^{-5}	0,00396	2.83×10^{-4}	0,02982
7200	3.32×10^{-5}	0,00345	3.10×10^{-4}	0,03267
8100			3.33×10^{-4}	0,03502
9000			3.45×10^{-4}	0,03633
48000				

The data shown in Figures 5C and 5D of the Article were obtained by using 3.8 g of the 0.1 M **pDoAO** gel containing **C_8Ac** at the concentration of 8×10^{-6} M. The gel-to-sol transitions were induced by adding 40 µL of 99% CH_3SO_3H to the gel. The sol-to-gel transitions were promoted by injecting 310 µL of NaOH 2 M. A volume of 40 mL of pure deionized water constituted the phase collecting the secretion of the artificial gland model **pDoAO+DM** in both its gel and sol state. The values of the

C_8Ac molar fraction ($\chi_{(C_8Ac)}$) secreted by the artificial gland model in both its gel and sol state were determined by recording the emission spectrum of **C_8Ac** from the aqueous solution contained in the beaker (see Figures S14 and S15). The method of calculation of $\chi_{(C_8Ac)}$ was explained above.

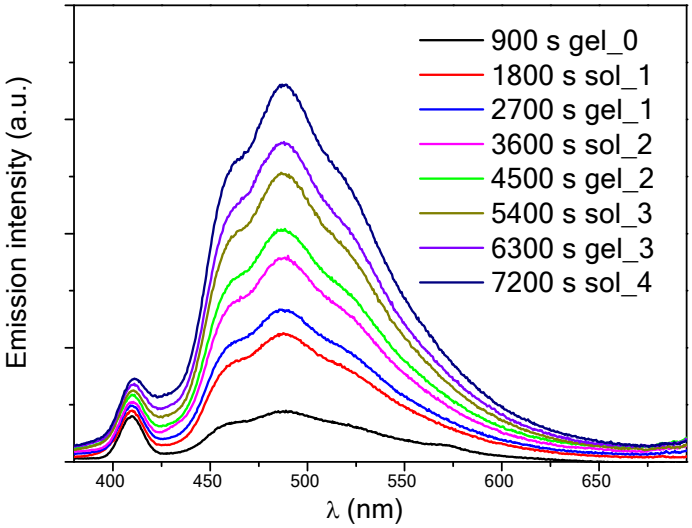

Figure S14. Emission spectra of **C_8Ac** secreted at different elapsed times in the collecting aqueous solution when **pDoAO+DM** was alternatively in the gel and sol states.

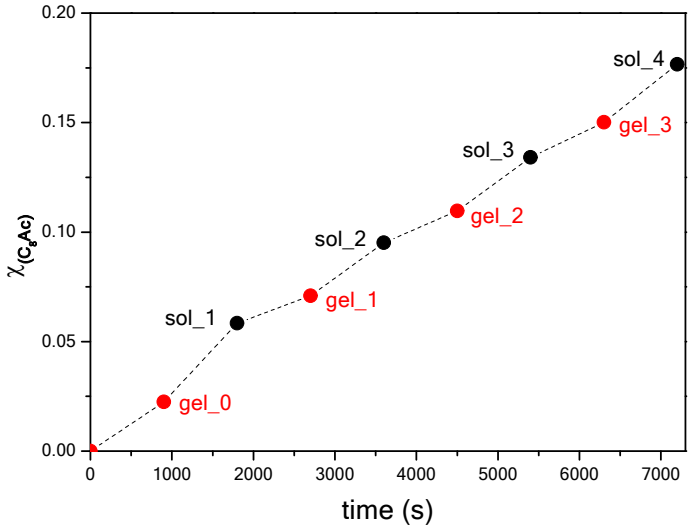

Figure S15. Trend of $\chi_{(C_8Ac)}$ in the aqueous solution collecting **C_8Ac** secreted by **pDoAO+DM** in its consecutive gel and sol states.

The values of the molar fraction of the surfactant molecules ($\chi_{(pDoAO)}$) released by the composite **pDoAO+DM** system was determined by recording the absorption spectra of the aqueous solution, and knowing the absorption coefficients values of **pDoAO** molecules in both its zwitterionic and cationic state (see Figures S16 and S17).

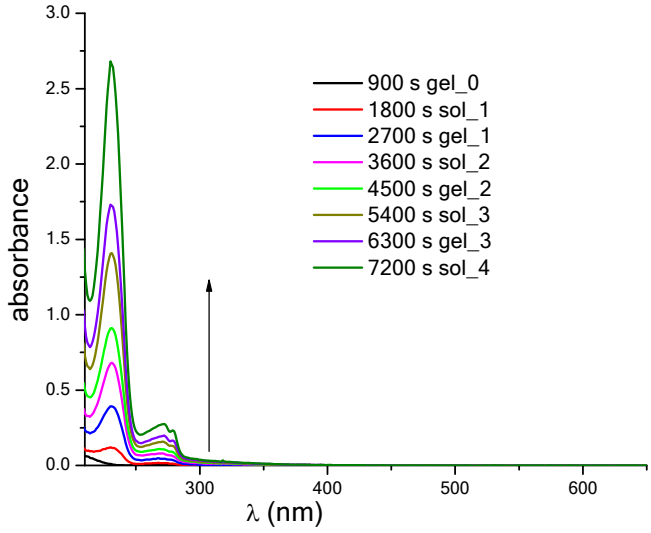

Figure S16. Absorption spectra of the collecting aqueous solution when **pDoAO+DM** was alternatively in its gel and sol states.

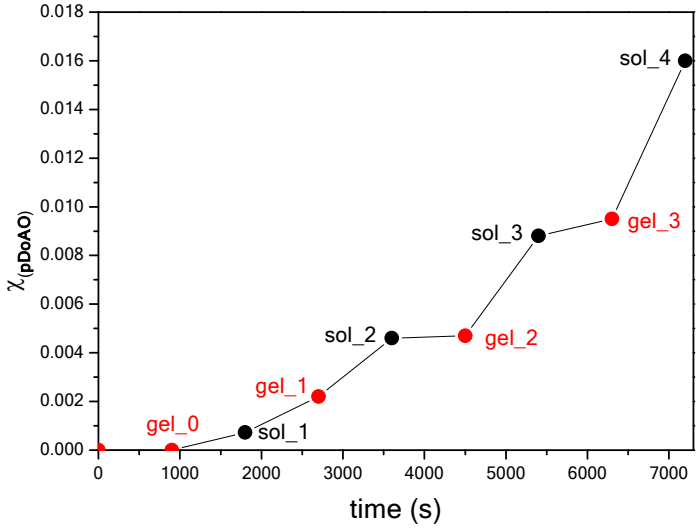

Figure S17. Trend of $\chi_{(pDoAO)}$ in the aqueous solution collecting the molecules released by **pDoAO+DM** in its consecutive gel and sol states.

*I.4 Contribution of the dialysis membrane to the composite **pDoAO+DM** system*

To monitor the contribution of the dialysis membrane (**DM**) with respect to the performances of the composite **pDoAO+DM** system, the releases of **C_8Ac** from aqueous solutions at different pHs, devoid of the **pDoAO** surfactant, and through the dialysis membrane, were investigated spectro-fluorometrically.

The experimental conditions that were common to all the experiments performed to monitor the role of **DM** are:

2 mL of aqueous solution with $[\mathbf{C_8Ac}]_{initial}$ = 8×10^{-6} M (internal solution) were separated by the dialysis membrane from 20 mL of water (collecting solution), maintained at 298 K and under constant magnetic stirring.

I) The internal solution was at pH=4 (after addition of CH_3SO_3H) and with $[\mathbf{C_8Ac}]_{initial}$ = $8x10^{-6}$ M.

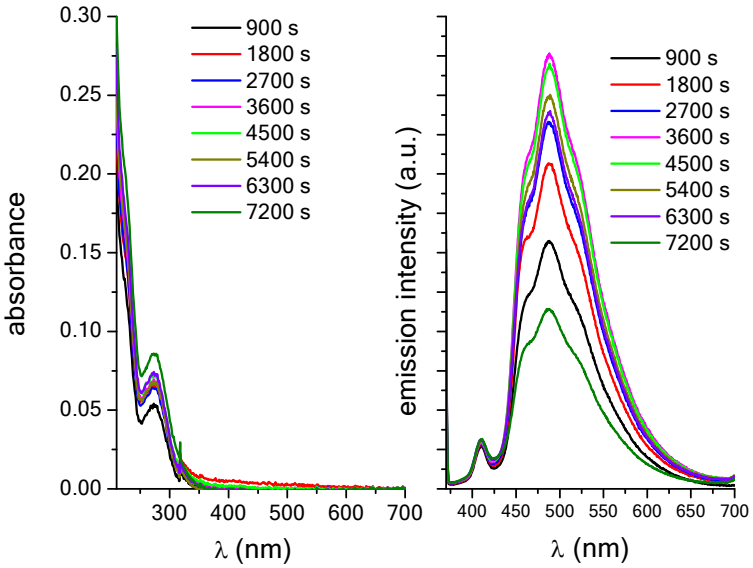

Figure S18. Absorption spectra (on the left) and emission spectra (on the right) of the collecting aqueous solution at different elapsed times (see the legends). The spectral contributions were originated by the **H_2O+DM** system with the internal aqueous solution at pH=4 and having $[\mathbf{C_8Ac}]_{initial}$ = 8×10^{-6} M.

II) The internal solution was at pH=8 (after adding NaOH) and with $[\mathbf{C_8Ac}]_{initial}$ = 8×10^{-6} M.

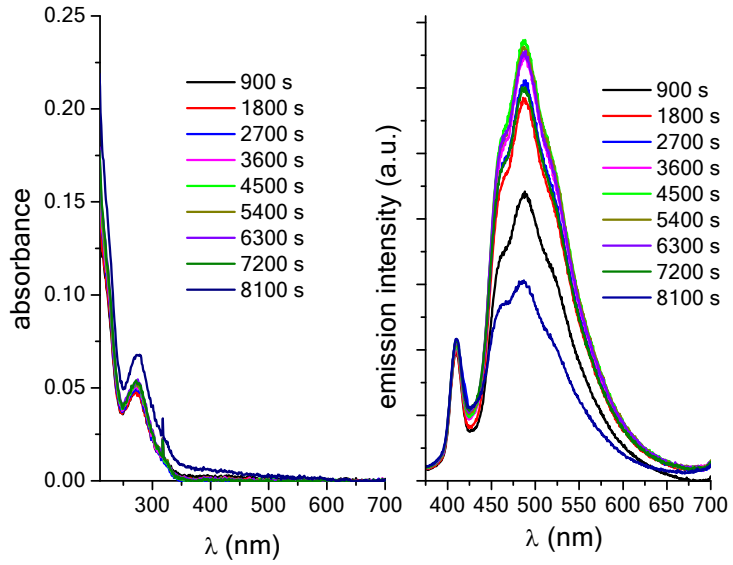

Figure S19. Absorption spectra (on the left) and emission spectra (on the right) of the collecting aqueous solution at different elapsed times (read the legends). The spectral contributions were originated by the **H_2O+DM** system with the internal aqueous solution at pH=8 and having $[\mathbf{C_8Ac}]_{initial} = 8\times10^{-6}$ M.

III) The internal solution was pure deionized water with $[\mathbf{C_8Ac}]_{initial} = 8\times10^{-6}$ M.

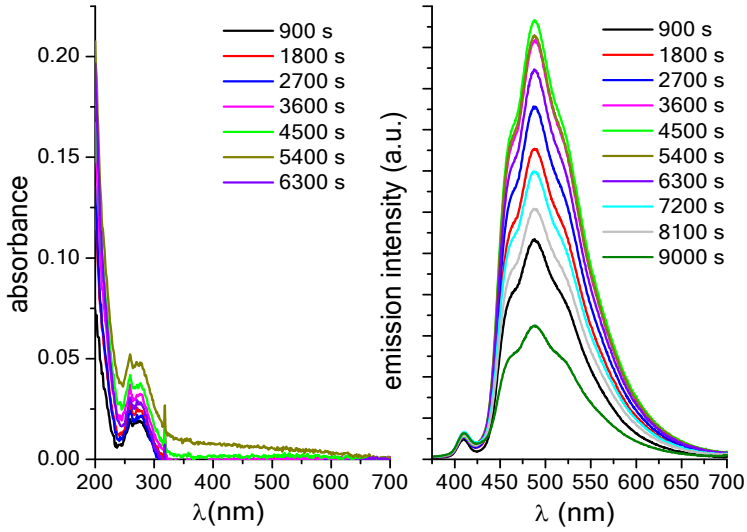

Figure S20. Absorption spectra (on the left) and emission spectra (on the right) of the collecting aqueous solution at different elapsed times (see the legends). The spectral contributions were

originated by the **H_2O+DM** system with the internal aqueous solution that was pure deionized water with $[\mathbf{C_8Ac}]_{initial} = 8\times10^{-6}$ M.

By using equation (2), the molar fractions of **C_8Ac** from the three solutions were calculated (see Figure S21). All the three trends show a bell curve. At first, **C_8Ac** was released by **DM**. Then, it was withdrawn.

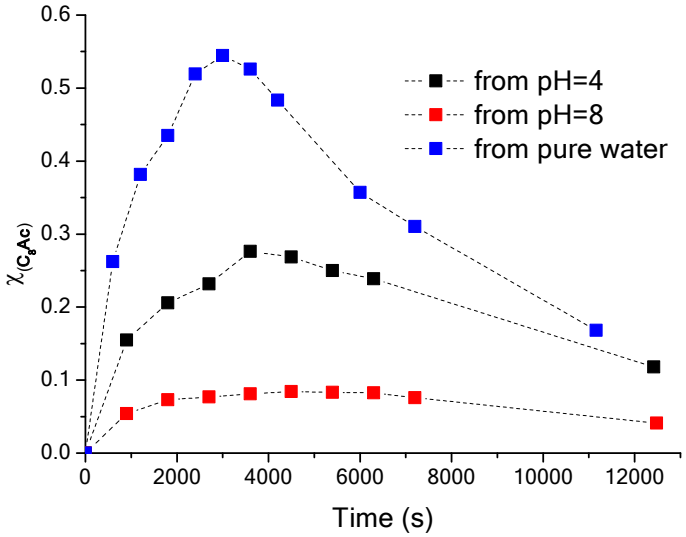

Figure S21. Trends of the molar fraction of **C_8Ac** collected in 20 mL of pure water and coming from 2 mL of aqueous solutions at different pHs.

To understand the origin of the "withdrawing" action, we performed experiments where the pH of both the internal and the collecting aqueous solution were adjusted.

IV) The internal and the collecting solutions were at pH=4 (after addition of CH_3SO_3H) and the internal solution had $[\mathbf{C_8Ac}]_{initial} = 8\times10^{-6}$ M.

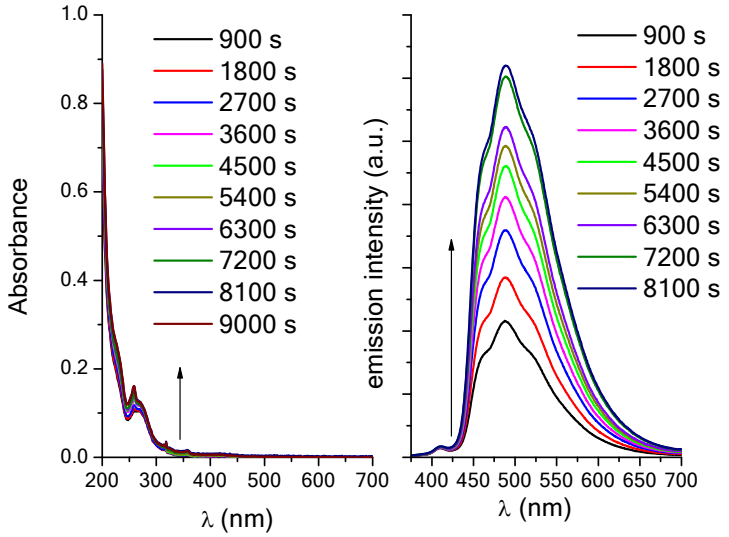

Figure S22. Absorption spectra (on the left) and emission spectra (on the right) of the collecting aqueous solution at different elapsed times. The spectral contributions were originated by the **H_2O+DM** system with the internal and collecting aqueous solution at pH=4. In the internal aqueous solution, the initial concentration of **C_8Ac** was 8×10^{-6} M.

V) The internal and the collecting solutions were at pH=8 (after addition of NaOH) and the internal solution had $[\mathbf{C_8Ac}]_{initial} = 8\times10^{-6}$ M.

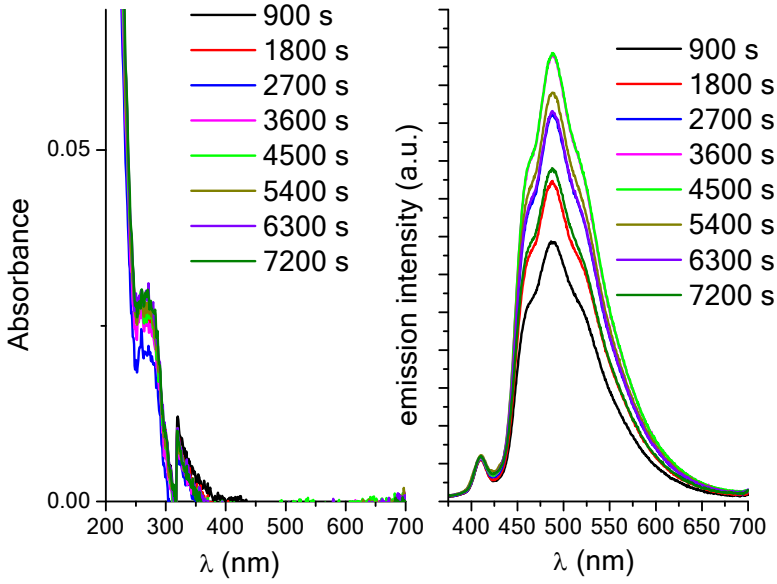

Figure S23. Absorption spectra (on the left) and emission spectra (on the right) of the collecting aqueous solution at different elapsed times. The spectral contributions were originated by the

H_2O+DM system with the internal and collecting aqueous solution at pH=8. In the internal aqueous solution, the initial concentration of **C_8Ac** was 8×10^{-6} M.

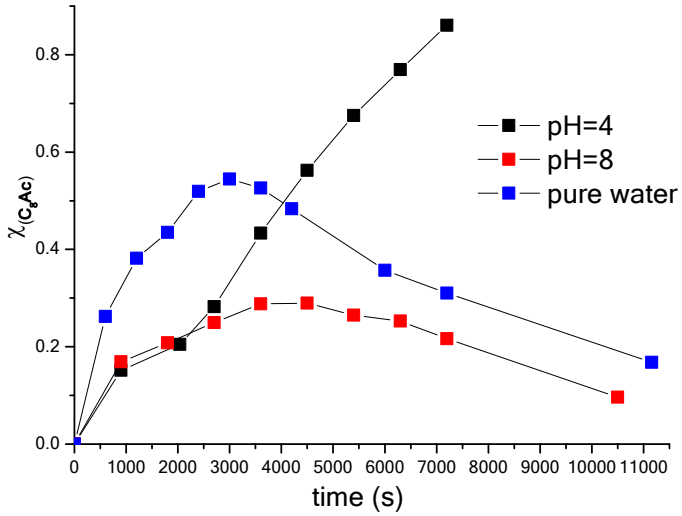

Figure S24. Trends of the molar fraction of **C_8Ac** released from 2 mL of water and collected in 20 mL of water. The pHs of both aqueous solutions were adjusted by addition of CH_3SO_3H to have pH=4, and NaOH to have pH=8.

From Figure S24, it is evident that only when both the internal and the collecting aqueous solutions were at pH=4, the trend of $\chi_{(C_8Ac)}$ grew monotonically and did not exhibit the "withdrawing" action. The origin of this behavior could be the slow release of a by-product by the dialysis membrane that becomes negatively charged. These negative charges withdraw **C_8Ac** and are responsible for the bell-shape of the trends shown in Figures S21 and S24. When the collecting solution is acid, the superficial negative charges of **DM** are neutralized. The by-product released by **DM** is responsible for the spectral bands recorded in absorption and shown in Figures S18, S19, S20, S22, and S23.

Comparisons:

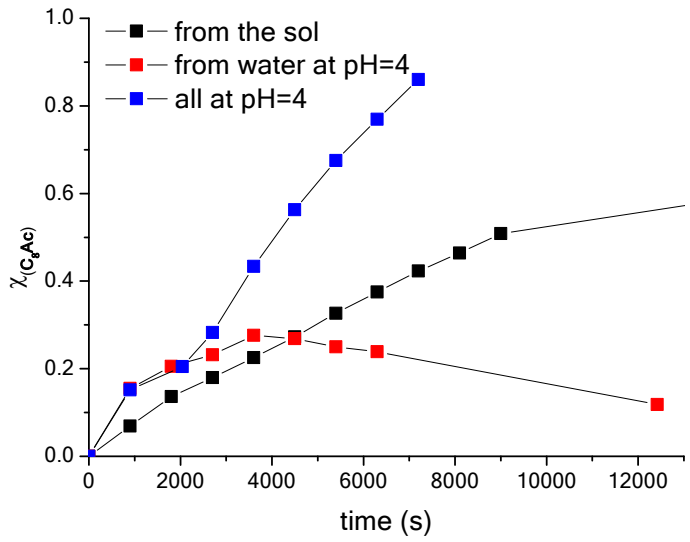

Figure S25. Trends of $\chi_{(C_8Ac)}$ vs. time from the composite **pDoAO+DM** system in the sol state (black points), and from **H_2O+DM** system when only the internal solution was at pH=4 (red points) and both aqueous solutions were acid (blue points).

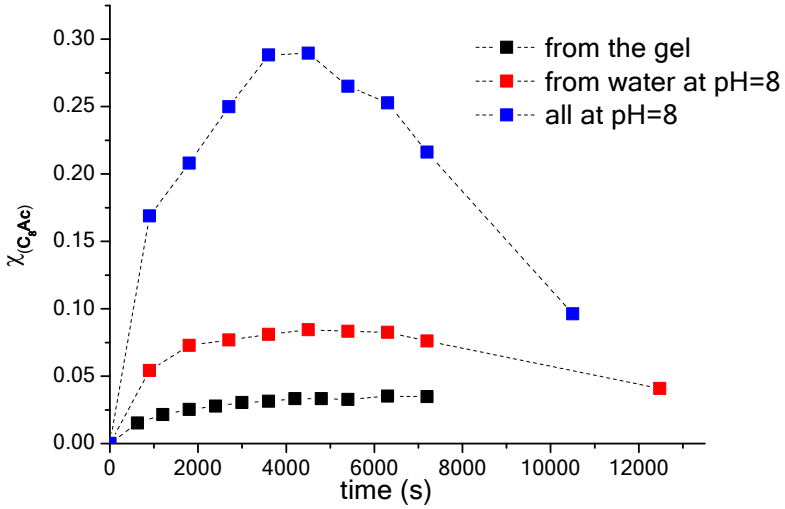

Figure S26. Trends of $\chi_{(C_8Ac)}$ vs. time from the composite **pDoAO+DM** system in the gel state (black points), and from **H_2O+DM** system when only the internal solution was at pH=8 (red points) and both aqueous solutions were alkaline (blue points).

From Figures S25 and S26 it is evident that the sol and gel states of **pDoAO** slow down the secretion of **C_8Ac.** Moreover, the surfactant **pDoAO** buffers the "withdrawing" action of the dialysis membrane. The latter action is particularly evident for the sol state when the surfactant molecules are positively charged after their protonation.

II. References

[1] U. Costas-Costas, C. Bravo-Diaz, E. Gonzalez-Romero, *Langmuir*, **2003**, *19*, 5197-5203.